Overexpression *Beadex* Mutations and Loss-of-Function *heldup-a* Mutations in Drosophila Affect the 3′ Regulatory and Coding Components, Respectively, of the *Dlmo* Gene

Michal Shoresh, Sara Orgad, Orit Shmueli, Ruth Werczberger, Dana Gelbaum, Shirly Abiri and Daniel Segal

Department of Molecular Microbiology and Biotechnology, Tel-Aviv University, Tel-Aviv 69978, Israel

Manuscript received April 13, 1998
Accepted for publication June 12, 1998

ABSTRACT

LIM domains function as bridging modules between different members of multiprotein complexes. We report the cloning of a LIM-containing gene from Drosophila, termed *Dlmo*, which is highly homologous to the vertebrate LIM-only (LMO) genes. The 3′ untranslated (UTR) of *Dlmo* contains multiple motifs implicated in negative post-transcriptional regulation, including AT-rich elements and Brd-like boxes. *Dlmo* resides in polytene band 17C1-2, where *Beadex* (*Bx*) and *heldup-a* (*hdp-a*) mutations map. We demonstrate that *Bx* mutations disrupt the 3′UTR of *Dlmo*, and thereby abrogate the putative negative control elements. This results in overexpression of *Dlmo*, which causes the wing scalloping that is typical of *Bx* mutants. We show that the erect wing phenotype of *hdp-a* results from disruption of the coding region of *Dlmo*. This provides molecular grounds for the suppression of the *Bx* phenotype by *hdp-a* mutations. Finally, we demonstrate phenotypic interaction between the LMO gene *Dlmo*, the LIM homeodomain gene *apterous*, and the *Chip* gene, which encodes a homolog of the vertebrate LIM-interacting protein NLI/Ldb1. We propose that in analogy to their vertebrate counterparts, these proteins form a DNA-binding complex that regulates wing development.

LIM domains constitute a novel subclass of cysteine-rich motifs and are found in various proteins involved in key processes during development and differentiation (reviewed in Curtiss and Heilig 1998; Dawid *et al.* 1998; Jurata and Gill 1998). They are composed of ~55 residues with the consensus sequence $CX_2CX_{16\text{-}23}HX_2CX_2CX_{16\text{-}23}CX_2C$ (where X is any amino acid), and they bind two atoms of Zn^{2+}. The "LIM" acronym is derived from the first three homeodomain proteins in which these domains were recognized: *l*in-11, which functions in asymmetric division of *Caenorhabditis elegans* secondary vulval blast cells (Freyd *et al.* 1990); *I*sl1, which binds to the rat insulin I gene enhancer (Karlsson *et al.* 1990) and has a major function in motor neuron development (Pfaff *et al.* 1996); and *m*ec-3, which is essential for differentiation of touch receptor neurons in *C. elegans* (Way and Chalfie 1988). LIM proteins often contain multiple (up to five) LIM domains in tandem. While originally identified in LIM homeodomain proteins, LIM proteins are also found to contain other known domains, such as kinase or GAP domains, as well as transcriptional activation domains (reviewed in Sanchez-Garcia and Rabbitts 1994; Taira *et al.* 1995). Still, other LIM proteins contain no additional domain of known function [LIM-only proteins (LMO)]. Despite the structural resemblance of the LIM domain to the GATA-1-type zinc finger, there is no evidence that LIM domains bind to DNA. Rather, growing evidence indicates that they mediate interaction with other proteins (Curtiss and Heilig 1998; Jurata and Gill 1998).

The nuclear localization of many LIM proteins and the fact that they often contain known transcriptional activation domains prompted the suggestion, and subsequently the demonstration, that the LIM domains play a role in modulation of the activity of the transcriptional activation domains associated with them. For example, the transcriptional activation capability of the amphibian LIM homeodomain protein Xlim-1 is relieved when its LIM domains are either deleted (Taira *et al.* 1994) or bound to the interacting protein NLI/Ldb1 (Agulnick *et al.* 1996; Breen *et al.* 1998). These observations suggest that the LIM domains of Xlim-1 negatively regulate its transcriptional activation activity. In other cases, LIM domains have been shown to positively regulate transcription activation activity. For example, the murine LIM homeodomain protein Lhx3 acts synergistically with the pituitary-specific POU homeodomain protein Pit-1 in activation of transcription from several pituitary-specific promoters (Bach *et al.* 1995). The association of these proteins is mediated by the LIM domains of Lhx3 and POU domains of Pit-1 (Bach *et al.* 1995).

Corresponding author: Daniel Segal, Department of Molecular Microbiology and Biotechnology, Tel-Aviv University, Tel-Aviv 69978, Israel. E-mail: dsegal@ccsg.tau.ac.il

LIM domains can also mediate binding of two LIM proteins resulting in homodimers, as in the case of the cysteine-rich protein (CRP; Feuerstein *et al.* 1994; Sanchez-Garcia *et al.* 1995) or in heterodimers, *e.g.*, CRP and Zyxin (Sadler *et al.* 1992; Schmeichel and Beckerle 1994).

LMO proteins serve to link different transcription factors that either contain or lack LIM domains. For example, two transcription factors, the zinc finger GATA-1 protein and the bHLH Tal1 protein, synergize in activating transcription from a target gene when they are bridged by the LIM domains of LMO2 (Wadman *et al.* 1997). A *N*uclear *L*IM-*I*nteracting protein (NLI, also termed Ldb1) has recently been shown to mediate binding of LIM proteins to their partners in various transcription complexes (Visvader *et al.* 1997; Breen *et al.* 1998; Jurata *et al.* 1998).

Certain LIM proteins are cytoplasmic (*e.g.*, Zyxin, CRP, CRIP, Paxillin, MLP; Curtiss and Heilig 1998; Jurata and Gill 1998). There they also serve as adaptor molecules between various cytoskeletal proteins. For example, Paxillin, which is found at focal adhesion sites, contains binding sites for Vinculin and for the focal adhesion tyrosine kinase FAK (Brown *et al.* 1996). Zyxin contains a proline-rich, α-actinin-binding domain (Crawford and Beckerle 1992), and MLP binds actin filaments (Arber and Caroni 1996). These interactions are mediated by the respective LIM domains.

Taken together, these *in vitro* studies demonstrate a role for LIM domains in the assembly of different proteins into functional transcription complexes or into higher-order components of the cytoskeleton.

Drosophila offers a unique opportunity to study the role of LIM proteins in the context of the whole organism and to identify by genetic means the proteins they interact with. Here we report the isolation of a LMO gene from Drosophila. The gene has been independently isolated by Zhu *et al.* (1995) and was termed *Dlmo*. We show that the 3′ untranslated region (UTR) of *Dlmo* contains various motifs [AT-rich elements (ARE) and Brd-like boxes] that have been implicated in negative post-transcriptional regulation of various genes. We demonstrate that hypermorphic mutations at the *Beadex* (*Bx*) locus disrupt the 3′UTR of *Dlmo*, leading to overexpression of the gene. Furthermore, we show that loss-of-function mutations at the adjacent *heldup-a* (*hdp-a*) locus represent lesions in the coding region of *Dlmo*, thus providing a molecular basis for the genetic interaction between *Bx* and *hdp-a* mutations. Finally, we demonstrate phenotypic interactions among mutations in *Dlmo*, in the *apterous* LIM homeodomain gene, and in the *Chip* gene, which is homologous to the vertebrate NLI protein. These observations suggest that in analogy to their vertebrate counterparts, these three proteins form a DNA-binding complex that regulates wing-specific genes.

MATERIALS AND METHODS

Drosophila stocks: Strains were maintained and crosses were conducted on cornmeal-molasses medium at 25°. For egg collection, flies were transferred to bottles attached to egg-laying plates (3% Bacto-agar, 2% sugar, 1.5 g/liter methylparaben) supplemented with live yeast paste at 25°. Description of balancer chromosomes and markers can be found in Lindsley and Zimm (1992). The Canton-S strain was used as a wild-type stock. The following strains were used: π_2 and *C(1)DX, yf*; π_2 (kindly provided by W. R. Engels), Bx^1, Bx^3, *Inscy w* Bx^M, *Inscy w* and *Df(1)N19/FM6* (provided by the Bloomington Stock Center), Bx^2, and *Dp(1:1)*Bx^r, *B* Bx^r,*car/C(1)DX, yf* and *C(1)DX, ywf* (provided by the Mid America Stock Center). Deficiency *Df(1)N19* deletes 17C1-2 to 18A1 and the cytology of *Dp(1;1)*Bx^r is 17A1-17A4; 17E1-17F3 (Lindsley and Zimm 1992). Strains used for interaction studies were as follows: *yw; Chip*$^{e5.5}$*/CyO, Df(2R)Kr*^{4}, Kr^{B80}, *Dp(1;2)*y^+ (kindly provided by D. Dorsett), ap^{56f}, *Dp(2;2)41A*, al^2 *cy* cn^2 L^4 sp^2/*In(2L)CyIn(2R)Cy*, and *pr cn Dp(2;Y)C* (obtained from the above-mentioned stock centers).

***P*-element-induced mutagenesis:** Males from the π_2 strain (Engels and Preston 1984) were crossed to females from the M strain *C(1)DX, y w f*. The resulting dysgenic male progeny were crossed in groups of 15–20 to *Df(1)N19/FM6* or Bx^3/Bx^3 tester females. Female offspring from these test crosses that exhibited the relevant phenotype (erect or scalloped wings in the first cross or normal wings in the second cross) were allowed to mate individually with their sibling males, and the resulting male offspring were crossed to compound-X *P* cytotype females, *C(1)DX,y f*; π_2, to establish a stable stock. To avoid clusters, only one line from each bottle of the cross was subsequently used for further analysis.

Classification of the scalloped wing phenotype: Wing margin abnormalities were routinely classified according to the number of notches at the anterior and posterior margins of the wing: rank 1, normal wings; rank 2, one to two notches at the posterior margin; rank 3, more than two notches at the posterior margin; rank 4, more than two notches at the posterior margin plus one to two notches at the anterior margin; rank 5, more than two notches at the posterior and anterior margin; rank 6, notches as in rank 5 plus blisters on the wing blade; rank 7, strap wings; rank 8, club wings (see Figure 5).

Standard DNA techniques: Restriction site mapping, Southern blotting, subcloning, library screening with ^{32}P-labeled probes, and isolation of genomic DNA were carried out essentially as described by Sambrook *et al.* (1989). The genomic library used was in λFIX II (Stratagene, La Jolla, CA).

PCR screen for LIM-containing genes: Genomic DNA, a cDNA library constructed from 0–4-hr-old embryos (courtesy of N. Brown), as well as cDNA generated from Canton-S embryos, larvae, pupae, or adults, were used as templates.

Partially degenerate primers were designed according to conserved amino acid sequences from the LIM domains of the Drosophila *apterous* gene and other LIM domain-containing proteins from vertebrates and plants (Baltz *et al.* 1992), taking into consideration the codon usage of Drosophila. The following primers were used:

P1: 5′AGACACTGCAGCAGAAGCAGTTGACGTGAAAAAC 3′
P2: 5′AACAAGAATTCTGGCGCGCATGAC 3′
P3: 5′TGCGGCGAGCTCATC/ACAGGAC/TCGCTA/TT/CC/TTCCTC 3′
P4: 5′GCTAACCTCGAGGTAA/GTCCCGT/CTTGCA 3′
P5: 5′CGAATTCTGCG/TCCGGCTGCGGC 3′

The designed primers had the potential to amplify a single LIM domain (primer pairs P3 + P4 or P5 + P4) or tandem

LIM domains (primer pairs P3 + P1, P5 + P1, P2 + P3, or P5 + P2). A variety of temperature ranges were used for annealing (37, 42, or 55°). Amplified fragments were subcloned in pBluescript and sequenced at the sequencing unit of Tel-Aviv University.

Northern analysis: PolyA$^+$ RNA was prepared from 0–4-hr-old embryos of different genotypes using the mRNA purification kit of Pharmacia (Piscataway, NJ). ^{32}P-labeled riboprobes were synthesized using the 1.8-kb cDNA of *Dlmo* and *rp49* as templates. Northern blots were quantified using ImageMaster DTS and ImageMaster 1D software (Pharmacia).

***In situ* hybridization:** *In situ* hybridization to larval imaginal discs was performed according to the method of Tautz and Pfeifle (1989). The 1.8-kb cDNA clone of *Dlmo* was labeled with digoxigenine (Boehringer Mannheim, Indianapolis) and used as a probe. We took special care to perform the procedure on the discs of all strains simultaneously and under the same conditions. Discs were mounted in glycerol and photographed.

PCR analysis of mutants: Genomic DNA was used for long and short PCR reactions. Long PCR was performed using the Expand Long Template PCR System (Boehringer Mannheim), and short PCR was performed using *Taq* polymerase (Appligene) according to the manufacturer's instructions. The following set of 17 primers was designed according to the sequence of the 1.8-kb cDNA of *Dlmo* and of adjacent genomic sequences: primer 1, nt 4–26; primer 2, nt 173–186; primer 3, nt 360–383; primer 4, nt 4011–4033; primer 5, nt 79–101; primer 6, nt 275–295; primer 7, nt 518–540; primer 8, nt 649–661; primer 9, nt 841–860; primer 10, nt 938–960; primer 11, nt 1027–1046; primer 12, nt 1041–1061; primer 13, nt 1328–1350; primer 14, nt 1549–1568; primer 15, nt 2098–2117; primer 16, nt 3230–3253; primer 17, nt 6401–6425.

For each primer, the position of the corresponding sequence is given according to the numbering in Figure 2 of Zhu *et al.* (1995). Primers corresponding to downstream and upstream genomic sequences also follow this numbering. Note that primers 5 and 6 correspond to exon Ib in Zhu *et al.* (1995). The orientation of the primers is indicated in Figure 2B.

Two primers were designed according to 5′ and 3′ ends of the *P* element:

5′ *P* element: 5′ATACTTCGGTAAGCTTGCGCTATC3′
3′ *P* element: 5′CATACGTTAAGTGGATGTCTCTTG3′

PCR fragments were cloned into the pGEM-T-vector (Promega, Madison, WI), when deemed necessary, and were sequenced.

RESULTS

Isolation of *Dlmo* and the structure of its 3′UTR: Various combinations of partially degenerate PCR primers, designed according to conserved LIM sequences, were used to amplify single or tandem LIM domains from templates of either genomic DNA, an embryonic cDNA library, or cDNA of different developmental stages of *Drosophila melanogaster*. One PCR-amplified fragment, produced from an embryonic cDNA template using primers P3 and P4 (see materials and methods), was found upon sequencing to contain a novel LIM consensus motif. This PCR fragment was used as a probe to isolate cDNA clones from a 3–12-hr-old embryonic cDNA library. A 1.8-kb embryonic cDNA clone was isolated and sequenced. It was found to comprise 1798 nucleotides capable of encoding a 266-amino acids-long protein with two tandem LIM motifs and no homeodomain or any other known domain. Thus, it is a LMO protein. While this work was in progress, the same sequence was reported by Zhu *et al.* (1995), who termed it Drosophila LMO (*Dlmo*). Our cDNA contains exons 2–5, identified by Zhu *et al.* (1995). The first LIM domain of the conceptual *Dlmo* protein is 79 and 69% similar to the first LIM domain of the human LMO1 and LMO2, respectively, whereas the second LIM domain of *Dlmo* is 94 and 60% similar to the second LIM domain of the human counterparts, respectively.

The structure of the 776-nucleotide-long 3′UTR of *Dlmo* has particular bearing on the analysis of mutants in this gene (described below). It contains four $AT_{3\text{-}5}A$ boxes, seven AT_3 motifs, and several stretches of Ts, the longest of which is T_{12}, collectively referred to as ARE (see Figure 1), which in various eukaryotic genes increase destabilization of the transcript (Chen and Shyu 1995). In addition, the 3′UTR of *Dlmo* contains five $AGT_{3\text{-}4}A$ sequences (Figure 1) that are closely related to the Drosophila Brd box (AGCTTTA). Brd boxes also mediate negative post-transcriptional regulation, probably by conferring instability upon the transcript (Lai and Posakony 1997). Thus, the 3′UTR of *Dlmo* may be involved in negative regulation of *Dlmo*.

***Bx* mutations affect the 3′UTR of *Dlmo*:** The 1.8-kb *Dlmo* cDNA was used as a probe to isolate genomic clones from a λFIX Drosophila genomic library. Three partially overlapping clones were isolated. *In situ* hybridization to polytene chromosomes using the 1.8-kb *Dlmo* cDNA as a probe indicated that the gene maps to band 17C on the *X* chromosome (data not shown). This is in accord with the mapping by Zhu *et al.* (1995). The 17C region has been previously the subject of chromosomal walks, and a total of nearly 250 kb of genomic DNA from this region have been isolated and physically mapped (Mattox and Davidson 1984; Mariol *et al.* 1987). Comparison of the published restriction maps from these walks with the map derived from the three genomic phage clones we have isolated indicated potential overlap. Southern analysis of genomic clones from the walk (clones 13, 24, and 19; Figure 4 in Mattox and Davidson 1984; kindly provided by W. Mattox) probed with the 1.8-kb *Dlmo* cDNA verified that *Dlmo* is contained within the genomic sequences included in these clones (Figure 2A).

Several genes are known to reside in the 17BC region (FlyBase; Lindsley and Zimm 1992). Of these, recessive mutations in *hdp-a* (causing erect wings) and dominant mutations in *Bx* (causing scalloping of the wing margin) have been previously mapped to a 0.4-kb *Bam*HI fragment within that part of the 17C chromosomal walk, which we have shown to overlap *Dlmo*. Because much of the 3′UTR of *Dlmo* resides within a 0.4-kb *Bam*HI fragment (Figure 1), we examined whether *hdp-a* or *Bx* mutations localize to it. Five *Bx* mutants are available

Figure 1.—Nucleotide sequence of the 3′UTR of *Dlmo*. Numbering is according to the sequence in Zhu *et al.* (1995). The stop codon is in lowercase letters. The two putative polyadenylation signals are in bold letters. The two *Bam*HI sites and the position of primers 14 and 15 used in Figure 3 are indicated. The ARE motifs and the T stretch are boxed. Brd-like boxes are underlined. The proximal breakpoint of the deletion in three of the *Bx* mutants is indicated by dotted lines. Primer 13, which delimits the coding region, is indicated.

(*Bx*^{1}, *Bx*^{2}, *Bx*^{3}, *Bx*^{J}, and *Bx*^{M}), all of which are insertional mutants of different transposable elements (Mattox and Davidson 1984), but all previously described *hdp-a* mutants have been lost.[1] We have performed PCR reactions using primers flanking the 0.4-kb *Bam*HI fragment in the 3′UTR of *Dlmo* (Figure 1), as well as genomic DNA from these five *Bx* mutants as templates. These reactions amplified a fragment longer than the expected 0.4-kb fragment from each of the *Bx* mutants (Figure 3). These results indicate that *Bx*^{1}, *Bx*^{2}, and *Bx*^{J} contain inserts ~8 kb long, and *Bx*^{3} and *Bx*^{M} contain inserts 9 and 14 kb long, respectively, within the 0.4-kb *Bam*HI fragment of the 3′UTR of *Dlmo*. The sizes of the inserts in these mutants are in agreement with the results of Mattox and Davidson (1984), which were derived from restriction mapping and Southern analysis. These results demonstrate that *Bx* mutations localize to *Dlmo*.

[1] The mutant designated *hdp-a*^{102} in FlyBase is not uncovered by the chromosomal deletion *Df(1)N19*; hence, is not an allele of *hdp-a* and should be renamed (data not shown).

The inserts in the *Bx* mutations analyzed disrupt the 3′UTR of *Dlmo*. We hypothesize that these mutations may exert their phenotypic effect by interfering with the function of the putative negative regulatory motifs present in the 3′UTR, resulting in overexpression of the *Dlmo* transcript. A critical prediction of this hypothesis is that removal of these motifs from the 3′UTR of *Dlmo* would result in a mutant phenotype characteristic of insertional *Bx* mutations.

To produce deletions in *Dlmo* that might result in *Bx*-like wing scalloping, and in the hope of generating new *hdp-a* mutations, we mobilized *P* elements in the wild-type π_2 strain by hybrid dysgenesis. This strain contains multiple copies of *P* element, one of which maps to 17C2-3 (O'Hare and Rubin 1983). Hybrid dysgenesis in π_2 has been shown to be an effective means for producing *Bx* and *heldup* mutants (Engels and Preston 1984), most of which were attributable to the *P* element in 17C2-3 (Simmons *et al.* 1984). Comparison of the sequence of the genomic 1.8-kb *Bam*HI fragment flanking the *P* element in 17C2-3 (O'Hare and Rubin 1983; courtesy of K. O'Hare) with the sequence of *Dlmo* indicates that this *P* element in π_2 resides 707 bp down-

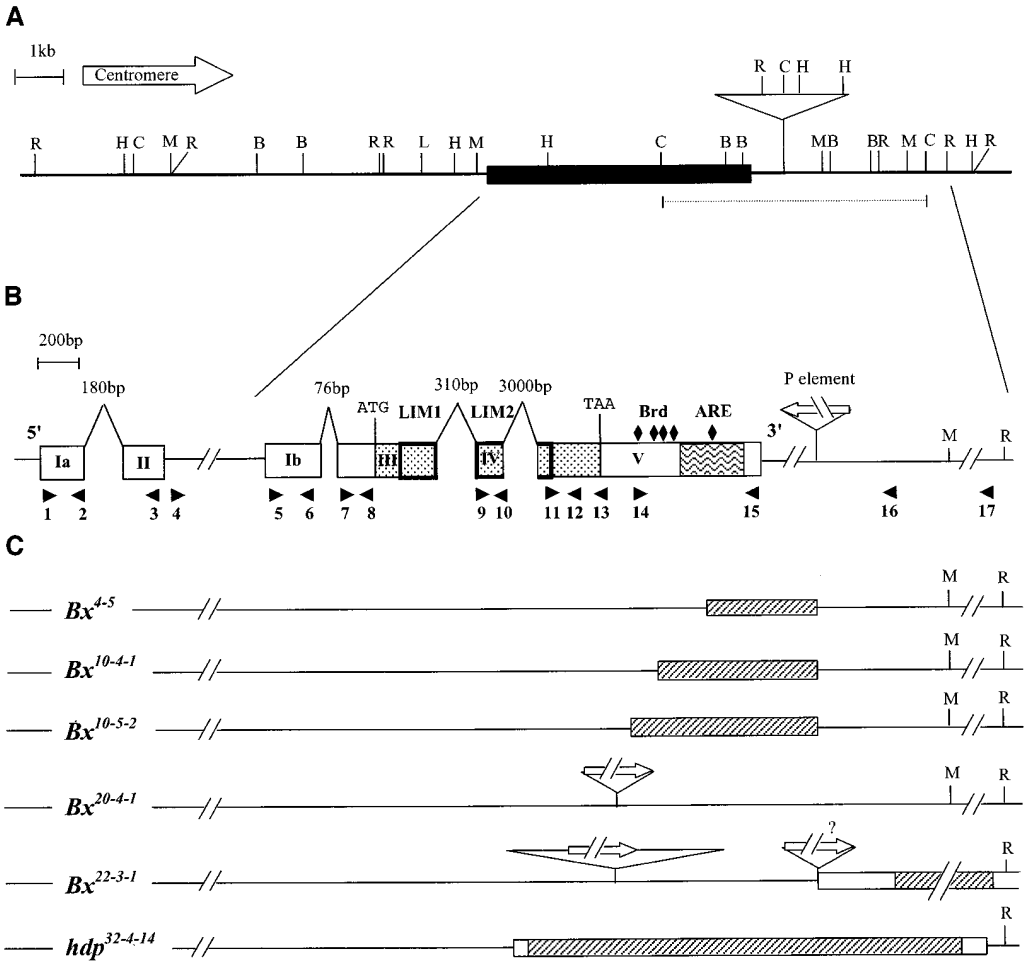

Figure 2.—Map of the *Dlmo* region at 17C. (A) The position of the *Dlmo* transcript (solid box) and the *P*-element insertion site are indicated on the restriction map of the region. Restriction sites are as follows: *Bam*HI, B; *Sac*I, C; *Eco*RI, R; *Sma*I, M; *Hin*dIII, H; *Sal*I, L. The dotted line indicates the *Sac*I fragment used as a probe for Southern analysis. (B) Enlargement of the map around the *Dlmo* gene. The exon (boxes)-intron (solid lines) organization of the *Dlmo* transcript is outlined. Exons Ia and II are not included in the map depicted in A. The coding region is indicated by the dotted boxes. The two LIM domains are enclosed in bold boxes, the ARE region is indicated in wavy lines, and the Brd-like boxes are shown as diamonds. Arrowheads depict position and direction of primers used for PCR analysis of *Bx* and *hdp* mutants. (C) Characterization of newly generated *Bx* alleles and *hdp-a* allele. Hatched boxes represent deleted sequences. Open boxes indicate potentially deleted sequences (exact breakpoint ends not determined). Positions of *P*-element insertions are shown for $Bx^{20\text{-}4\text{-}1}$ and $Bx^{22\text{-}3\text{-}1}$.

stream of the 3′ end of our cDNA, suggesting that deletions extending into *Dlmo* could be generated by imprecise excision of this *P* element.

Generation and characterization of new *Bx* mutants: Males from the π_2 strain were crossed to M cytotype *C(1)DX, y w f* females. The resulting dysgenic sons were crossed to *Df(1)N19/FM6* females (Figure 4, Cross A), and the ~60,000 *FM6*-bearing female progeny were screened for wing scalloping. To identify which of these may be *Bx* mutants, we used the following two criteria: (1) Wing scalloping in *Bx* mutants is suppressed when combined with a deletion of the 17BC chromosomal region. Flies heterozygous for such a deletion, *e.g.*, *Df(1)N19*, have normal wings. (2) *Bx* wing scalloping is augmented when combined with a chromosome carrying a duplication of the normal 17BC region. Flies heterozygous for such a duplication, *e.g.*, $Dp(1;1)Bx^{r}$, have normal wings and rarely display very mild scalloping (Lifschytz and Green 1979). We crossed *FM6*-bearing female progeny displaying scalloped wings to males carrying *Df(1)N19* and scored the female offspring for amelioration of the wing scalloping. Putative *Bx* mutants thus identified were subsequently crossed to $Dp(1;1)Bx^{r}$, and female offspring were scored for augmentation of wing scalloping. Based on these two criteria, 17 out of the 34 dominant *X*-linked wing scalloping mutants generated are *Bx* mutants (Table 1).

All 17 new *Bx* mutants are homozygous viable. The degree of wing scalloping varied between the different mutants, and they are listed in Table 1 in their order of severity. In each mutant, scalloping was more pronounced in the homozygotes than in the heterozygotes. We have classified scalloping according to its severity, where rank 1 is normal wing and rank 8 is a nearly strap-like wing (Figure 5; Table 1). We find that a population of flies carrying any *Bx* allele displays a characteristic distribution of severity ranks of wing scalloping. Suppression of scalloping in *Bx*/*Df(1)N19* was therefore recognizable as a shift in the distribution of the wing phenotypes toward the less severe ranks, as compared

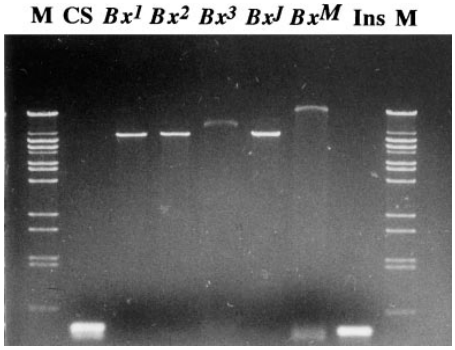

Figure 3.—PCR analysis of existing *Bx* alleles (Bx^1, Bx^2, Bx^3, and Bx^M) and two wild-type strains, Canton S (CS) and *Inscy w* (Ins), used to generate Bx^M. Primers 14 and 15 flanking the two *Bam*HI sites present in the 3′UTR of *Dlmo* were used (see Figure 1). λ*Bst*EII digest was used as size markers.

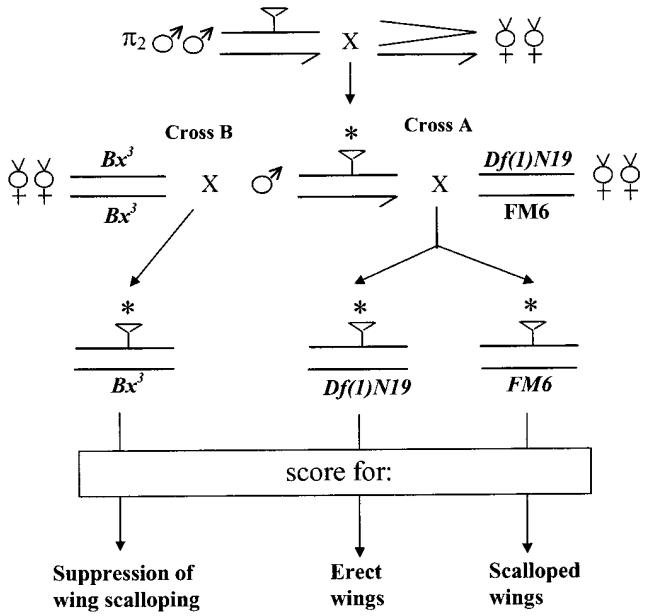

Figure 4.—Scheme of crosses used to produce mutants with erect wings and scalloped wings (Cross A) and suppressors of *Bx* (Cross B).

to *Bx*/+ (Figure 6). The suppressed phenotype appeared to be directly correlated to the severity of scalloping caused by the original *Bx* mutation. The milder the original scalloping was, the closer the suppressed phenotype was to wild-type wings (Table 1; Figure 6). Suppression was therefore barely noticeable for the mildest mutants, such as $Bx^{20\text{-}4\text{-}1}$, but was very conspicuous in more severe mutants, such as Bx^3, $Bx^{10\text{-}5\text{-}2}$, and $Bx^{4\text{-}5}$ (Figure 6). Likewise, augmentation of any *Bx* allele by $Dp(1;1)Bx^r$ was evident as a shift of the wing phenotypes toward the more severe ranks (Table 1; Figure 6). Here, too, the resulting phenotype appeared to be directly correlated to the severity of scalloping caused by the original mutation, and augmentation of scalloping was readily observed, even in the mildest mutants. For exam-

TABLE 1

Severity ranks of wing scalloping in different *Bx* mutants

	Severity of wing scalloping				
Bx mutant	*Bx/Bx*	*Bx/+*	*Bx/Df(1)N19*	$Bx/Dp(1;1)Bx^r$	$Bx/hdp^{32\text{-}4\text{-}14}$
13-4-1	7–8	6–7[a]	6	7	5–6
10-5-2	7–8	6–7	6	7	4
7-8-1	7	6–7	6	7	5–6
15-5-2	7	6–7	6	7	6
10-4-1	7	6–7	6	7	4
7-7-1	7	5	5–6	6	3
12-2-3	7	5	4–5	6	3–4
4-5	7	4–5	3–4	6–7	3–4
23-1-20	3–4	1–2	1	4–5	1
22-3-1	3–4	1–2	1	3–4	1
14-1-3	5[b]	1–2	1	3	1
12-3-36	3–4	1–2	1	3	ND
3-5-4	3	1–2	1	3	1
17-3	3	1–2	1	2	1
20-4-1	3–4	1[c]	1	4	1
16-7	3	1	1	3–4	ND
11-1-8	3	1	1	3	ND

The different mutants are listed in deceased order of severity. Each value represents the median of ≥100 flies scored. ND, not done.

[a] Smaller numbers represent severity ranks displayed by ~25% of the population.

[b] In $Bx^{14\text{-}1\text{-}3}$ homozygotes, the distribution around the median was exceptionally wide.

[c] In $Bx^{20\text{-}4\text{-}1}$/+ heterozygotes, ~90% of the population displayed rank 1 wing phenotype and 10% displayed ranks 2 and 3.

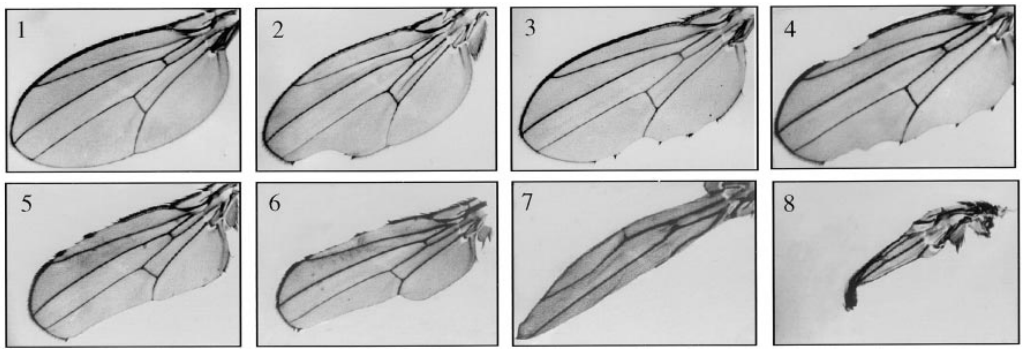

Figure 5.—Abnormal wing phenotype of *Bx* mutants. Wing margin severity defect was ranked according to the number of notches at the anterior and posterior margins of the wing (see materials and methods).

ple, marked augmentation of wing scalloping is seen for Bx^3 and the newly induced *Bx* alleles $Bx^{20\text{-}4\text{-}1}$ and $Bx^{4\text{-}5}$, but it is less evident for $Bx^{10\text{-}5\text{-}2}$.

These observations suggest that *Bx* mutations are hypermorphs and that the degree of severity of the *Bx*-engendered wing scalloping depends on the quantity of a certain gene product (see also Lifschytz and Green 1979). Taken together, these phenotypic results and our demonstration that *Bx* mutations interfere with the 3′UTR of *Dlmo*, which may negatively regulate the stability of the *Dlmo* transcript, suggest that this gene product is likely to be DLMO. We propose that the hypermorphic nature of these mutations results from overexpression of *Dlmo*, resulting from abrogation of negative control motifs in its 3′UTR.

Molecular analysis of *Bx* mutants: PCR and Southern analyses were performed on genomic DNA of 11 out of the 17 newly induced *Bx* mutants. Genomic DNA from the π_2 strain, used for generating these mutants, served as a control. The primers used for these reactions were designed according to sequences from the cDNA of *Dlmo* and from genomic sequences flanking the site of

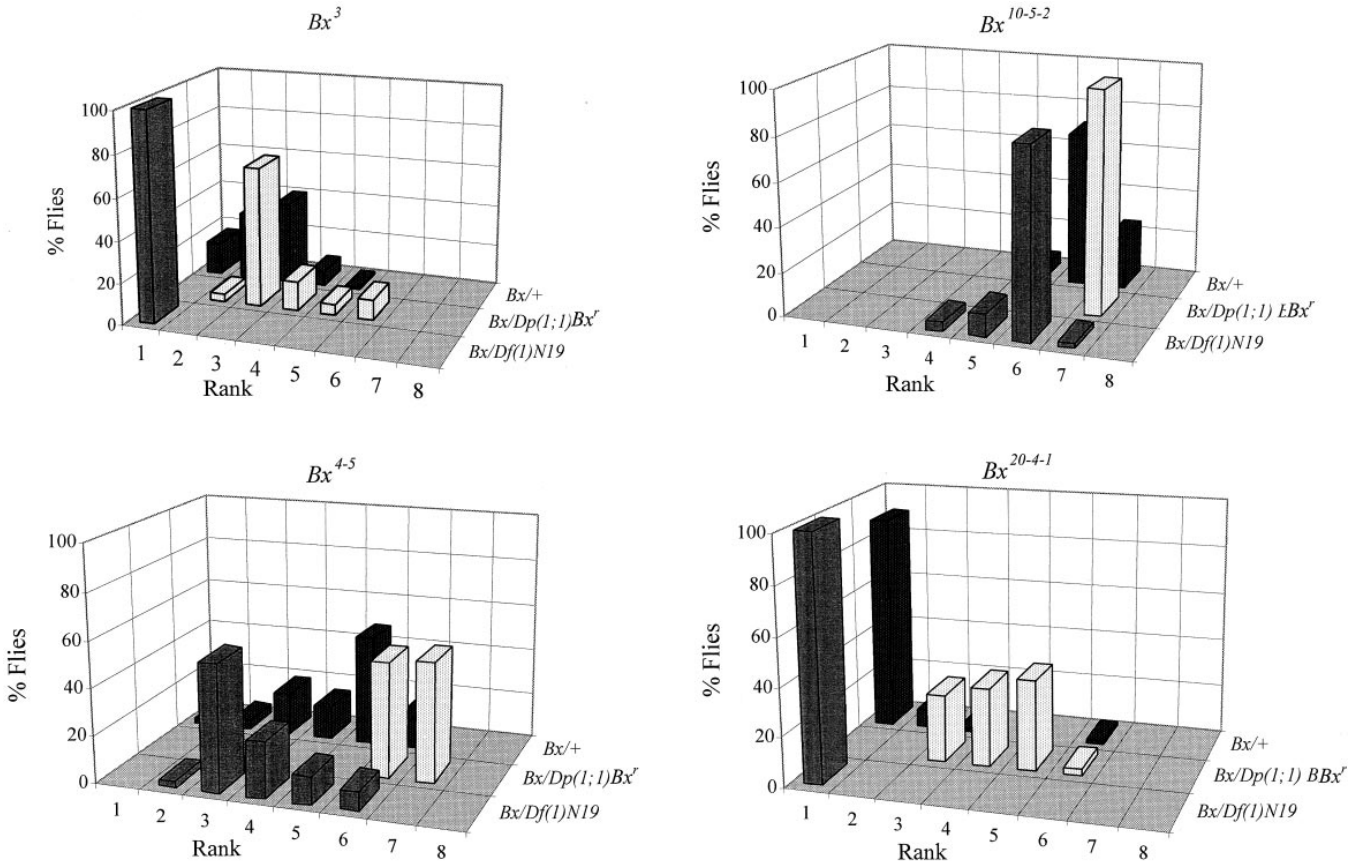

Figure 6.—Distribution of wing defects according to severity (see Figure 5) in the existing Bx^3 allele and in three newly generated *Bx* alleles, $Bx^{10\text{-}5\text{-}2}$, $Bx^{4\text{-}5}$, and $Bx^{20\text{-}4\text{-}1}$. Each histogram represents the distribution of wing scalloping in hetrozygous females and shows the suppression of this phenotype by *Df(1)N19* and augmentation by $Dp(1;1)Bx^r$. Approximately 100 flies were scored for each genotype.

	Primer pair					
Bx mutant	11+13	14+15	11+15	14+16	11+16	14+17
π_2	0.3kb	0.54kb	1.0kb	4.5kb	5.2kb	4.8kb
13-4-1	+[a]	-[b]	-	-	-	1.8kb[c]
10-5-2	+	-	-	-	0.8kb	nd[d]
7-8-1	+	-	-	-	nd	2.5kb
10-4-1	+	-	-	0.6kb	nd	nd
4-5	+	-	-	1kb	nd	nd
22-3-1	+	+	8.0kb	-	nd	-
3-5-4	+	+	+	+	nd	nd
17-3	+	+	+	1.6kb	nd	4.5kb
20-4-1	+	+	4.0kb	-	nd	-
16-7	+	+	+	+	nd	nd
11-1-8	+	+	+	+	nd	nd

[a] Fragment size is identical to that of π_2

[b] No PCR fragment amplified

[c] Size of PCR fragment which differs from this of π_2

[d] Not done

Gray boxes represent deviations from π_2

Figure 7.—PCR-amplified products from new *Bx* mutants.

insertion of the 17C2-3 *P* element in π_2 (see Figure 2B and materials and methods for exact location of the primers).

Interestingly, this analysis provides evidence that 8 of the 11 newly induced *Bx* mutants examined have lesions confined to the 3′UTR of *Dlmo* and the downstream flanking genomic sequences. For example, the mutants Bx^{4-5} and Bx^{10-4-1} amplified fragments that are 1 and 0.6 kb long, respectively, when using primer pair 14 + 16, while the π_2 control gave a 4.5-kb fragment, suggesting they have deletions in the region delimited by these primers (Figure 7). Likewise, the mutant Bx^{10-5-2} amplified a fragment 0.8 kb long when using primer pair 11 + 16, as compared to 5.2 kb in the control, suggesting it has a deletion in the region between their corresponding genomic sequences (Figure 7). In the mutants Bx^{7-8-1} and Bx^{13-4-1}, the primer pair 14 + 17 amplified fragments 2.5 and 1.8 kb long, respectively, while the corresponding control fragment is 7.7 kb long. Given that the π_2 strain has a 2.9-kb *P* element inserted 0.7 kb downstream of *Dlmo* (Figure 2A; O'Hare and Rubin 1983), the sizes of the deleted genomic fragments in these mutants, excluding the *P* element, are as follows: Bx^{4-5}, 0.6 kb; Bx^{10-4-1}, 1 kb; Bx^{10-5-2}, 1.5 kb; Bx^{7-8-1}, 2.3 kb; and Bx^{13-4-1}, 3 kb. In the mutant Bx^{7-7-1}, no fragments were amplified using any primer pair downstream of primer 13, which delimits the 3′ end of the coding region, even when using the most downstream primer available, primer 17 (Figure 7). This indicates that the deletion in Bx^{7-7-1} extends downstream beyond sequences corresponding to primer 17 (Figure 2B). Taken together, in each of these six *Bx* mutants, the deletion removes part of the 3′UTR of *Dlmo*, but leaves the coding region of the gene intact. We have confirmed these results by Southern analysis (data not shown).

To get a more accurate estimate of the extent of the deletions, we cloned and sequenced the PCR fragments of the mutants Bx^{4-5} and Bx^{10-4-1} amplified using primer pair 14 + 16, and the fragment of Bx^{10-5-2} amplified using primer pair 11 + 16 (Figure 7). Sequence analysis has confirmed that the deletion in each of these mutants extends from the site of the *P*-element insertion in the π_2 strain, removing the *P* element entirely, into the 3′UTR of *Dlmo*. The portion of the 3′UTR sequences deleted is different in the three mutants. In Bx^{4-5}, the last 226 bp of the 3′UTR of *Dlmo* are missing, including one ATTTA motif, the T stretch, and one Brd-like box (Figure 1). In Bx^{10-4-1}, an additional 126 bp have been

TABLE 2

Distribution of severity ranks of wing scalloping in *Bx* mutants lacking parts of the 3′UTR of *Dlmo*

	Rank of severity of wing scalloping						
Bx mutant	1	2	3	4	5	6	7
10-5-2					5	70	25
10-4-1					20	56	24
4-5	2	4	19	14	47	13	

Values are the percentages of flies displaying a given severity rank in a population of ≥100 heterozygous *Bx*/+ females scored.

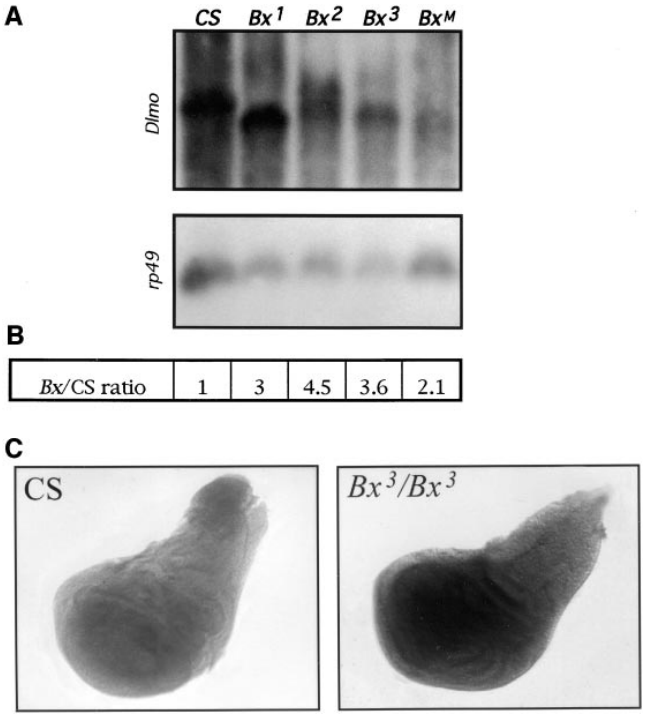

Figure 8.—Expression of *Dlmo* in *Bx* mutants. (A) Northern analysis of wild-type, Canton S (CS), and four insertional *Bx* mutants. Poly(A)$^+$ RNA was extracted from 0- to 4-hr-old embryos and probed with *Dlmo* cDNA. The bottom panel shows the reprobing with *rp49* as a loading control. (B) Ratio of *Dlmo* transcript (*Bx*/CS) normalized according to *rp49*. (C) Expression pattern of *Dlmo* in wild-type (CS) and Bx^3 mutant wing imaginal discs.

deleted from the 3′UTR, removing all ARE motifs and four Brd-like boxes (Figure 1). In $Bx^{10\text{-}5\text{-}2}$, the deletion is larger, leaving only the first 107 bp of the 3′UTR and removing all the putative negative regulatory elements present in the 3′UTR of *Dlmo* (Figure 1). Taken together, the PCR and sequence analyses of these *Bx* mutants support the hypothesis that the *Bx* mutant phenotype results from abrogation of the 3′UTR of *Dlmo*. Interestingly, the extent of the deleted segment from the 3′UTR of *Dlmo* in these mutants is directly correlated with the severity of their wing scalloping, where $Bx^{10\text{-}5\text{-}2}$ has the most severe phenotype, $Bx^{10\text{-}4\text{-}1}$ is less severe, and $Bx^{4\text{-}5}$ is the mildest of the three (Table 2). In addition, the 3′UTR DNA lesions in $Bx^{10\text{-}4\text{-}1}$ and $Bx^{10\text{-}5\text{-}2}$ differ only in that the former lacks an additional Brd-like box. This may provide functional evidence that Brd-like boxes in *Dlmo* have a negative regulatory role.

The PCR products amplified from the mutants $Bx^{22\text{-}3\text{-}1}$ and $Bx^{20\text{-}4\text{-}1}$ using primer pair 11 + 15 (8 and 4 kb, respectively) were longer than the corresponding fragment in π_2 (1 kb, Figure 7), indicating that sequences ~7 and 3 kb long, respectively, have inserted into the fifth exon of the *Dlmo* gene in each of these mutants. Because the PCR product of primer pairs 14 + 15 and 11 + 13 in these mutants has the same size as in the control (Figure 7), we deduce that the inserts in these two mutants are localized to the 179-bp region between the sequences corresponding to primers 13 and 14, in the 5′-most portion of the 3′UTR of *Dlmo* (Figures 1 and 2C).

To further characterize the insertions in these two mutants, we used primers designed according to the 5′ and 3′ ends of the *P*-element sequences, in combination with primer 11 (Figure 2B; see materials and methods). The combination using the 5′ primer of the *P* element yielded fragments of 2 kb in the mutant $Bx^{22\text{-}3\text{-}1}$ and of 0.5 kb in the mutant $Bx^{20\text{-}4\text{-}1}$. These findings support the conclusion that in both mutants, the insertion was in the interval mentioned above. In the mutant $Bx^{22\text{-}3\text{-}1}$, the insertion consists of an excised *P* element with 1.7 kb of flanking genomic sequences at its 5′ end and 2.5 kb of flanking genomic sequences at its 3′ end (Figure 2C). In mutant $Bx^{20\text{-}4\text{-}1}$, the insertion consists of the *P*-element sequences only (Figure 2C).

In addition, no fragment was amplified using primer pair 14 + 16 in these two mutants. On the other hand, normal size fragments were amplified from their DNA using either primer pair 14 + 15 or the primer pairs located upstream to them. This suggests that in addition to the insertion, they have lesions removing sequences downstream of *Dlmo*, leaving its coding region intact (Figure 2C).

The mutants $Bx^{3\text{-}5\text{-}4}$, $Bx^{16\text{-}7}$, and $Bx^{11\text{-}1\text{-}8}$ had no visible difference from the control π_2 strain in all primer pairs used. Because of the limited resolution of the PCR technique, we cannot exclude the possibility that they have small lesions in the *Dlmo* gene that are responsible for their wing scalloping. This should be resolved by sequencing.

***Dlmo* expression is affected in *Bx* mutants:** Northern analysis of poly(A)$^+$ RNA extracted from 0–4-hr-old embryos of several *Bx* mutants (Bx^1, Bx^2, Bx^3, and Bx^M) and a control strain (Canton-S) was performed using the 1.8-kb cDNA of *Dlmo* as a probe. A 2.0-kb transcript exists in the control strain, while all *Bx* mutants examined have a truncated transcript that is ~0.5 kb shorter (Figure 8A). The longer transcript in Bx^2 may be the result of

TABLE 3

Distribution of severity ranks of wing scalloping in females transheterozygous for Bx^3 and newly induced *hdp-a* alleles

	Rank of severity of wing scalloping				
Genotype	1	2	3	4	5
$Bx^3/+$	30	32	38		
$hdp\text{-}a^{32\text{-}4\text{-}14}/Bx^3$	100				
$hdp\text{-}a^{26\text{-}3\text{-}7}/Bx^3$	88	10	2		
$hdp\text{-}a^{28\text{-}3\text{-}3}/Bx^3$	70	22	8		
$hdp\text{-}a^{28\text{-}1\text{-}5}/Bx^3$	70	21	9		
$hdp\text{-}a^{13\text{-}7\text{-}13}/Bx^3$	63	37			
$hdp\text{-}a^{9\text{-}4\text{-}1}/Bx^3$	48	41	11		
$hdp\text{-}a^{15\text{-}5\text{-}1}/Bx^3$	38	25	34		3
$hdp\text{-}a^{7\text{-}5\text{-}4}/Bx^3$	28	40	25	4	3

Values are the percentages of flies displaying a given severity rank in a population of ≥100 flies scored. $Bx^3/+$ is shown for comparison.

transcription termination within the gypsy element (see discussion).

To correct for the amounts of poly(A)$^+$ RNA loaded in each lane, the membrane was rehybridized with a probe of the ribosomal protein RP49. Scanning for quantification of the *Dlmo* RNA and the *rp49* RNA and normalizing for RNA loading indicated that the *Dlmo* transcript is overexpressed (two- to fourfold) in the *Bx* mutants as compared to the wild-type strain (Figure 8B).

Because the *Bx* phenotype is manifested in the wing, we compared the expression of *Dlmo* in the wing imaginal discs of Bx^3/Bx^3 and the wild-type Canton-S. The overexpression of *Dlmo* observed in the mutant embryos (Figure 8, A and B) is also evident in their discs (Figure 8C), which display stronger staining.

Generation and characterization of *hdp-a* mutants: All *hdp-a* mutants that have been generated previously were lost. The fact that *hdp-a* mutants suppress the wing scalloping phenotype of *Bx* mutants (Lifschytz and Green 1979) prompted us to try and generate new *hdp-a* alleles, by hybrid dysgenesis, to study the molecular basis underlying this interaction.

Two phenotypic criteria were used to identify recessive *hdp-a* mutants: (1) uncovering of the *hdp-a* mutation by *Df(1)N19* and (2) the ability of *hdp-a* mutants to suppress the dominant wing scalloping of *Bx*. These two strategies were used to screen for *hdp-a* mutants.

Strategy 1: Approximately 30,000 *Df(1)N19*-carrying female offspring from Cross A were screened for the erect wing phenotype (Figure 4). Six such independent mutants were recovered, and they were subsequently confirmed to be *X*-linked, recessive, and homozygous viable. We crossed the six erect wing mutants to Bx^3 and observed amelioration of wing scalloping in the female offspring of four ($hdp\text{-}a^{7\text{-}5\text{-}4}$, $hdp\text{-}a^{15\text{-}5\text{-}1}$, $hdp\text{-}a^{9\text{-}4\text{-}1}$, and $hdp\text{-}a^{13\text{-}7\text{-}13}$, Table 3). These four mutants do not complement each other, and all transheterozygous combinations of them display erect wings. These results suggest that these four mutants represent lesions in the *hdp-a* gene.

Strategy 2: Dysgenic males were crossed to Bx^3/Bx^3 females, and their female offspring were scored for suppression of the dominant wing scalloping (Figure 4, Cross B). Approximately 10,500 chromosomes were screened, and 20 such independent, *X*-linked *Bx* suppressors were isolated. These could correspond to lesions in *hdp-a* or in other second-site *Bx*-suppressor genes. Four of the *Bx* suppressors ($hdp\text{-}a^{32\text{-}4\text{-}14}$, $hdp\text{-}a^{26\text{-}3\text{-}7}$, $hdp\text{-}a^{28\text{-}1\text{-}5}$, and $hdp\text{-}a^{28\text{-}3\text{-}3}$) also have a recessive erect wing phenotype that is uncovered by *Df(1)N19*. These results suggest that they have lesions in *hdp-a*. All four mutants do not complement each other for the erect wing phenotype, nor do they complement the four *hdp-a* mutants generated in strategy 1. We conclude that these four *Bx* suppressors are *hdp-a* alleles, comparable to the *hdp-a* mutants generated in strategy 1.

Ranking the severity of the erect wing phenotype in these eight *hdp-a* mutants was difficult. The severity of the *hdp-a* mutants was easier to measure by determining the extent of their suppression of the wing scalloping of *Bx* mutants. The different degrees of severity of the eight *hdp-a* mutants, using this criterion, are depicted in Table 3. These *hdp-a* mutants also suppress the wing scalloping of the 17 newly generated *Bx* mutants (see Table 1 for suppression of the new *Bx* alleles by $hdp\text{-}a^{32\text{-}4\text{-}14}$), supporting the conclusion that they are indeed new *Bx* alleles.

Based on the degree of suppression of Bx^3, the $hdp\text{-}a^{32\text{-}4\text{-}14}$ allele is the most severe *hdp-a* allele in our collection.

***hdp-a* mutants represent loss of function of *Dlmo*:** Given the close proximity of *Bx* and *hdp-a* mutations on the genetic map (0.0045 map units, Lifschytz and Green 1979) and their phenotypic interaction, we were interested to examine what gene in the vicinity of *Dlmo* is affected by *hdp-a* mutations.

PCR analysis was performed on the $hdp\text{-}a^{32\text{-}4\text{-}14}$ allele, which was shown to suppress completely the wing scalloping phenotype of Bx^3 using primer pairs covering the entire *Dlmo* transcript (Figure 2B). All primer pairs corresponding to exons Ia, II, Ib, III, and IV amplified fragments identical in size to those amplified in the parental strain π_2 (data not shown). When primer pairs designed according to sequences corresponding to exon V were used, however, no amplified fragments were obtained. These results indicate that exon V was entirely absent in this *hdp-a* mutant, resulting in the loss of approximately half of the coding sequence of *Dlmo*, including part of the second LIM domain (Figure 2C). Another PCR reaction using primer 16, which is located downstream of the insertion site of the *P* element, in combination with primer 9, located in exon IV, indicated that the deletion in this mutant extends beyond the insertion site of the *P* element (Figure 2C).

TABLE 4

Genetic interaction of *Dlmo* with *ap* and *Chip*

Genotype	Severity of wing scalloping
$Bx^3/+$	Defective wings (rank 3)
$ap^{56f}/+$	Normal wings (rank 1)
$Chip^{e5.5/+}$	Normal wings (rank 1, rarely *Chip*-like nicks)
Df(Dlmo)/+	Normal wings (rank 1)
Dp(Dlmo)/+	Normal wings (rank 1, rarely rank 2)
$Dp(ap^+)/+$	Normal wings (rank 1)
$Df(Dlmo)/+;\ ap^{56f}/+$	Normal wings (rank 1)
$Dp(Dlmo)/+;\ ap^{56f}/+$	Defective wings (rank 3)
$Bx^3/+;\ ap^{56f}/+$	Defective wings (rank 5–6)
$Dp(Dlmo)/+;\ Dp(ap^+)/+$	Defective wings (rank 6)
$Bx^3/+;\ Dp(ap^+)/+$	Defective wings (rank 6–7)
$Df(Dlmo)/+;\ Chip^{e5.5}/+$	Normal wings (rank 1, rarely *Chip*-like nicks)
$Dp(Dlmo)+;\ Chip^{e5.5}/+$	Defective wings (rank 5–6)
$Bx^3/+;\ Chip^{e5.5}/+$	Defective wings (rank 6)
$ap^{56f}+/+\ Chip^{e5.5}$	Defective wings (severe *Chip*-like nicks)

Df(Dlmo) = *Df(1)N19*; *Dp(Dlmo)* = $Dp(1;1)Bx^r$; $Dp(ap^+)$ = *Dp(2;2)41A*.

Additional evidence supporting this conclusion was obtained from Southern analysis of $hdp\text{-}a^{32\text{-}4\text{-}14}$ using either the 1.8-kb cDNA of *Dlmo* or a genomic 5.9-kb *Sac*I fragment as a probe (Figure 2A).

Thus, the loss-of-function nature of the $hdp\text{-}a^{32\text{-}4\text{-}14}$ mutation results from disruption of the coding region of *Dlmo*. This result, combined with the overexpression of *Dlmo* in *Bx* mutants, provides molecular grounds for explaining the phenotypic interaction between *Bx* and *hdp-a* mutations.

***Dlmo* interacts genetically with *ap* and *Chip*:** The LIM motifs in LIM proteins function in protein-protein binding and, in some cases, mediate LIM-LIM interaction between different LIM proteins (Curtiss and Heilig 1998; Jurata and Gill 1998). In Drosophila, recessive mutations in the LIM homeodomain gene *apterous* (*ap*) cause truncated wings. The *ap* gene has been shown to be a key regulator of wing development (Cohen *et al.* 1992). Because both *Dlmo* and *ap* contain LIM domains and both affect wing development, we examined whether they interact. We generated various *Bx-ap* double heterozygotes and examined the morphology of their wings. The results are summarized in Table 4.

Double heterozygotes for overexpression mutations of *Dlmo* and for loss-of-function mutations of *ap* exhibit abnormal wing morphology markedly different from the phenotype of either of the two mutants alone. For example, slight overexpression of *Dlmo* combined with an *ap* mutation results in conspicuous augmentation of wing scalloping (*Dp(Dlmo)*/+; *ap56f*/+, rank 3, *vs.* *Dp(Dlmo)*/+, rank 1–2). Further increase in overexpression of *Dlmo* in *ap* heterozygotes leads to dramatic enhancement of wing scalloping ($Bx^3/+$; $ap^{56f}/+$, rank 5–6). The synergistic effect of *Bx* and *ap* mutations suggests that *Dlmo* and *ap* interact during wing development.

We further examined how manipulation of the levels of these gene products affects the wings. Heterozygotes for loss of function of both *Dlmo* and *ap* have normal wings (*Df(Dlmo/+*; $ap^{56f}/+$, rank 1). Likewise, elevated levels of ap^+ [*e.g.*, three doses in $Dp(ap^+)/+$ or four doses in *Dp(2;Y)C*; *Dp(2;2)41A*/+] do not affect wing morphology (rank 1, Table 4; M. Shoresh and D. Segal, unpublished observations, respectively). However, when combined with slight or marked overexpression of *Dlmo*, the elevated levels of ap^+ augment the wing scalloping of *Bx* [*e.g.*, *Dp(Dlmo)*/+; $Dp(ap^+)/+$, rank 6, and $Bx^3/+;\ Dp(ap^+)/+$, rank 6–7]. These results corroborate the conclusion that *Dlmo* and *ap* interact during wing development, and they imply that this interaction is sensitive to the dosage of their gene products.

In vertebrates, the NLI protein (also called Ldb1) has been shown to mediate the binding of LIM proteins to various transcription factors (Agulnick *et al.* 1996; Visvader *et al.* 1997; Breen *et al.* 1998; Jurata and Gill 1998). Recently, the Drosophila homolog of NLI, called *Chip*, has been isolated (Morcillo *et al.* 1997). Interestingly, loss-of-function mutants of *Chip* cause, in single doses, very mild nicks in the posterior wing margin (Morcillo *et al.* 1997). This phenotype is distinct from the *Bx* or *ap* wing scalloping. The CHIP protein binds *in vitro* the LIM domains of AP (Morcillo *et al.* 1997), and the *ap-Chip* interaction (*e.g.*, $ap^{56f}+/+\ Chip^{e5.5}$) results in dramatic truncation of the wing blade (Table 4; Morcillo *et al.* 1997). Given these observations and the fact that *Dlmo* is a LIM-containing gene that interacts with *ap*, we wanted to examine whether *Chip* mutants and *Dlmo* mutants interact. Reduction in the level of

Dlmo does not affect the loss-of-function *Chip* phenotype (*Df(Dlmo)*/+; $Chip^{e5.5}$/+; Table 4); however, elevation of the level of *Dlmo* in the *Chip* mutants (*e.g.*, in Bx^{3}/+; $Chip^{e5.5}$/+) results in a synergistic effect on wing development (rank 6). These results suggest that *Chip* and *Dlmo* interact, and this interaction is sensitive to the relative dosage of their gene products.

These phenotypic interactions indicate that *ap*, *Dlmo*, and *Chip* share a role in the regulation of wing margin development in Drosophila. The *in vitro* binding of AP and CHIP and the analogy to their vertebrate counterparts collectively suggest that these three proteins form a DNA-binding complex regulating wing-specific genes.

DISCUSSION

LIM-containing genes in Drosophila: The *Dlmo* gene belongs to a growing family of animal and plant genes encoding LIM proteins. LIM proteins have key roles in diverse processes during development and differentiation (Curtiss and Heilig 1998; Dawid *et al.* 1998; Jurata and Gill 1998). The LIM-containing genes identified to date in Drosophila exemplify the diverse and pivotal roles of LIM proteins. The *apterous* (*ap*), *islet* (*isl*), and *Arrowhead* (*Awh*) genes all encode, in addition to the LIM domains, a homeodomain, and are thus likely to be transcription factors. The *ap* gene is a key regulator of dorso-ventral patterning in the wing (Diaz-Benjumea and Cohen 1993; Blair *et al.* 1994) and is required for specification of embryonic muscle precursors (Bourgouin *et al.* 1992). In addition, *ap* is expressed in the embryonic central nervous system (CNS) and is required for projection of axons along their appropriate pathways (Lundgren *et al.* 1995). *ap* has also been implicated in neuroendocrine regulation of adult reproduction (Altaratz *et al.* 1991; Ringo *et al.* 1991). The vertebrate homolog of *ap*, *Lhx2*, is expressed in the embryonic nervous system, and mice homozygous for a null *Lhx2* mutation display massive brain defects (Porter *et al.* 1997). The Drosophila *isl* gene, like its vertebrate homologs, *Islet-1* and *Islet-2*, is expressed in a subset of embryonic motor neurons and interneurons, and loss of its function causes defects in axon pathfinding and targeting (Pfaff *et al.* 1996; Thor and Thomas 1997). The *Awh* gene is required for the establishment of a subset of imaginal tissues, the abdominal histoblasts, and the salivary imaginal rings (Curtiss and Heilig 1997). In addition, two homologs of the vertebrate cytoplasmic muscle LIM proteins (MLP) have been cloned from Drosophila, *Mlp60A*, and *Mlp84B*. No mutants have been described so far in either of these two genes; however, accumulating data suggest that like their vertebrate homologs, the Drosophila *Mlp* genes have a role in myogenesis (Stronach *et al.* 1996). Thus, key roles of LIM proteins appear to have been conserved from insects to mammals (Curtiss and Heilig 1998; Dawid *et al.* 1998; Jurata and Gill 1998).

Dlmo is the sole LMO gene identified so far in Drosophila (Zhu *et al.* 1995). On the other hand, the family of vertebrate LMO genes includes three genes, LMO1, LMO2, and LMO3 (Foroni *et al.* 1992). They function in mammalian hematopoiesis and, like the LIM homeodomain proteins, appear to play a role in transcription as they localize to the nucleus and associate with other known transcription factors (Curtiss and Heilig 1998; Dawid *et al.* 1998; Jurata and Gill 1998).

Negative regulatory elements in the 3′UTR of *Dlmo*: The 3′UTR of *Dlmo* contains multiple AREs and five Brd-like boxes. AREs are found in the 3′UTR of many mRNAs that code for proto-oncogenes, nuclear transcription factors, and cytokines (for reviews see Chen and Shyu 1995; Ross 1995; Abler and Green 1996). They represent the most common determinant for RNA stability in eukaryotic cells. Numerous studies in various *in vivo* and *in vitro* systems have shown that deletion or disruption of AREs results in more stable mRNAs, whereas the addition of AREs to the 3′ of reporter genes causes destabilization of the transcript. The mechanisms by which AREs direct mRNA degradation and the *cis*- or *trans*-acting factors involved are largely unknown. Thus, the AREs in the 3′UTR of the *Dlmo* gene are likely to be involved in negative post-transcriptional regulation. Interestingly, like their Drosophila homolog, the mammalian LMO1 and LMO2 genes contain AREs in their 3′UTR (McGuire *et al.* 1989; Royer-Pokora *et al.* 1991).

In addition to the AREs, the 3′UTR of *Dlmo* contains five heptanucleotide AGTTTTA sequence motifs that are closely related to the AGCTTTA motif, termed Brd box, found in the 3′UTR of the *Bearded* (*Brd*) gene and in many genes involved in Notch signaling during cell fate specification in the adult peripheral nervous system of Drosophila (Lai and Posakony 1997; Leviten *et al.* 1997). One of the five Brd-like boxes in the 3′UTR of *Dlmo* is located within the interval containing the AREs, whereas the remaining four are located upstream. The Brd boxes have been shown to be negative regulatory elements (Lai and Posakony 1997).

***Bx* lesions abrogate negative regulatory elements in the 3′UTR of *Dlmo*:** The results presented in this article demonstrate that the genetically defined *Bx* locus corresponds to the 3′UTR of *Dlmo*. Insertion of a *P* element or a retrotransposon in the 3′UTR of *Dlmo* can result in a dominant wing scalloping phenotype similar to that caused by removal of most or all the AREs and Brd-like boxes in the 3′UTR. We therefore surmise that the insertions into the 3′UTR of *Dlmo*—by retrotransposons or *P* elements or by deletion of parts of the 3′UTR of *Dlmo*—similarly abrogate the negative regulatory effect of the ARE and Brd-like motifs. Consequently, the level of the *Dlmo* transcript in the *Bx* alleles examined is two- to fourfold higher than that of the wild type, as expected if the ARE and Brd-like boxes had an RNA-destabilizing effect (Chen and Shyu 1995; Lai and Posakony 1997).

Transcriptional up-regulation caused by regulatory elements in the transposon can be ruled out because a similar hypermorphic phenotype is exhibited in Bx mutants lacking the 3′UTR region. In addition, we find correlation between the extent of the 3′UTR sequences missing in the three deletion-associated alleles and the severity of their wing scalloping.

Similar effects of transposon insertions on 3′UTR negative regulatory motifs have been reported for two other mutants in Drosophila. The dominant gain-of-function mutation Ser^D in the *Serrate* (*Ser*) gene results from insertion of the Tirant retrotransposon in the 3′UTR of *Ser*, causing termination of the transcript in Ser^D within the transposon's long terminal repeat, at a AAUAAA hexanucleotide that probably serves as a polyadenylation signal (Thomas *et al.* 1995). As a consequence of this premature termination, the *Ser* transcript is shorter by 600 nucleotides, which contain eight AREs. The *Ser* transcript and protein were found to be more abundant in the Ser^D mutant than in the wild type. The higher level of *Ser* transcript was shown to result from greater stability of the transcript in the mutant rather than from higher rate of transcription (Thomas *et al.* 1995).

A second example is the insertion of the blood retrotransposon in the 3′UTR of the *Brd* gene, which causes a dominant gain-of-function phenotype (Levi ten *et al.* 1997). Lai and Posakony (1997) have demonstrated that the 3′UTR of the *Brd* gene confers negative regulatory activity on heterologous reporter genes *in vitro* and in transgenic flies, and this activity is strongly dependent on the integrity of the Brd boxes. This indicates that *Brd* is normally regulated negatively by these boxes. The nullifying effect of the blood insert on the RNA-destabilizing activity of the *Brd* boxes is caused by premature termination of *Brd* transcription, resulting in a transcript lacking two of the three *Brd* boxes. This affects both *Brd* RNA and protein levels.

The *Dlmo* transcript in Bx^1, Bx^2, Bx^3, and Bx^M is ~0.5 kb shorter than in the wild type. Insertion of various retrotransposons, including copia and gypsy, in different genes in Drosophila causes premature termination of transcription of the host gene (for a review see Smi t h and Corces 1991). Transcription often terminates in polyadenylation signals present in the retrotransposon, as has been proposed for the Ser^D mutation (Thomas *et al.* 1995). In other cases, the retrotransposon insert was shown to potentiate the utilization of an upstream cryptic polyadenylation signal (Dorsett 1990). A cryptic polyadenylation signal is located immediately after the translation stop signal in the 3′UTR of *Dlmo* (Figure 1). Therefore, retrotransposons inserted in the 3′UTR of *Dlmo* in the Bx^1, Bx^2, Bx^3, and Bx^M mutants may cause truncation of the transcript by either of these means. In Bx^2, we observed, in addition to the truncated *Dlmo* transcript, a transcript larger than the wild type. In this mutant, the shorter transcript may represent termination at the cryptic polyadenylation signal, and the larger one may represent termination within the transposable element. Given the resolution of the Northern blot, it is not possible to determine which of these two alternative mechanisms operates in each of these *Bx* alleles. At any rate, the truncated *Dlmo* transcript is devoid of most if not all of the 3′UTR negative regulatory motifs. A polyadenylation signal is located in the *P* element 150 nucleotides downstream of its 5′ end. Therefore, the *P*-element insertions in $Bx^{20\text{-}4\text{-}1}$ and $Bx^{22\text{-}3\text{-}1}$ may have an effect similar to that of the retrotransposons in abrogating the negative regulatory elements in the 3′UTR of *Dlmo*. Likewise, the *Dlmo* transcript in the deletion-associated alleles $Bx^{4\text{-}5}$, $Bx^{10\text{-}4\text{-}1}$, and $Bx^{10\text{-}5\text{-}2}$ lacks most if not all of its 3′UTR. In these mutants, the *Dlmo* transcript may terminate at the cryptic polyadenylation site in the beginning of its 3′UTR. Alternatively, because the centromere-proximal breakpoint of these deletions is at the site of the *P*-element insertion in the π_2 strain, it is possible that *Dlmo* transcription terminates in sequences that are centromere proximal to this site. Indeed, we find that a polyadenylation signal resides 380 nucleotides downstream of the *P*-insertion site in π_2.

Overexpression of *Dlmo* causes wing scalloping: The *Bx* wing scalloping can be brought about by supernumerary copies of the normal 17BC chromosomal region, each likely having the normal *Dlmo* gene along with its control regions. This suggests that the abnormal wing morphology results from overexpression of the gene in those cells in which it is normally expressed, albeit at lower levels, rather than from spatial or temporal misexpression. A similar wing scalloping is brought about by *Bx* mutations that cause overexpression of the *Dlmo* gene. Therefore, we assume that *Dlmo* is expressed under its normal spatial-temporal control in these mutants also. This assumption is corroborated by the similar pattern of distribution of the *Dlmo* transcript in wild-type and *Bx* mutant imaginal discs, except that in the latter, the level of the transcript appears elevated. Thus, the scalloped wing phenotype is exclusively the result of disruption or deletion of the 3′UTR of the gene. Because wing scalloping is the only overt mutant phenotype in *Bx* mutants, whether heterozygous or homozygous, the overexpression of *Dlmo* apparently does not interfere with functions in which the *Dlmo* product may participate in cells, other than those at the wing margin. It will be interesting to examine the consequences of directed misexpression of *Dlmo* in cells or stages where it is not normally expressed because LMO proteins serve as bridges between different proteins (Cur tiss and Heilig 1998; Dawid *et al.* 1998; Jurata and Gill 1998).

***heldup-a* mutations correspond to loss-of-function of *Dlmo* and interact with *Bx*:** Recessive *hdp-a* mutations have been genetically mapped to close proximity (0.0045 map units) centromere distal of *Bx* mutations. Furthermore, *hdp-a* mutations have been reported to suppress in one dose the dominant wing scalloping of *Bx* mutations either in *cis* or in *trans* (Lifschytz and

Green 1979). Based on these observations, the hypermorphic nature of *Bx* mutations has been proposed to result from overexpression of a nearby structural gene, possibly *hdp-a* (Lifschytz and Green 1979; Mattox and Davidson 1984). Although all previously existing *hdp-a* alleles have been lost, we were able to regenerate *hdp-a* mutants in two ways, and both groups recapitulate the two characteristics of the previous alleles, namely erect wings and suppression of the dominant wing scalloping of *Bx* mutants. Molecular analysis has been carried out on one of them, $hdp\text{-}a^{32\text{-}4\text{-}14}$, demonstrating that it has a deletion of a major part of the coding region of *Dlmo*, including part of the second LIM domain, suggesting that *hdp-a* corresponds to loss-of-function of *Dlmo*. This conclusion is supported by the results obtained by Mattox and Davidson (1984) from restriction mapping and Southern analysis of one of the previously existing *hdp-a* alleles. They found that $hdp\text{-}a^{D30r}$ harbors a small deletion extending from the insertion site of the *P* element in π_2, removing the 0.4-kb fragment to which *Bx* mutations have been mapped and extending upstream of it. Comparison to the map of *Dlmo* suggests that the deletion in $hdp\text{-}a^{D30r}$ has removed part of the coding region of *Dlmo*. Loss of function of *Dlmo* could be also caused by mutations disrupting the promoter region of the gene.

Assuming that *hdp-a* mutations cause loss of the functional *Dlmo* product, we can explain in molecular terms the suppression of the *Bx* dominant wing scalloping by recessive *hdp-a* mutations. We propose that in *Bx* mutants, the *Dlmo* product is overexpressed because of abrogation of the negative control elements in its 3′UTR. Likewise, duplications of the normal 17BC region result in excess of the *Dlmo* protein, causing in turn a scalloping phenotype comparable to that of *Bx* mutants. When either of these duplications or *Bx* mutations are combined with a deletion of the chromosomal 17BC region or with *hdp-a* mutations, which likely cause loss of function of *Dlmo* protein, the net amount of the *Dlmo* product is reduced to approximately the wild-type level, resulting in normal wing morphology.

The anatomical cause for the erect wings in *hdp-a* mutants is unknown at this time. Mutations in many genes in Drosophila affect wing posture. Most of them affect either components of the wing muscles or their innervation (reviewed in Bernstein *et al.* 1993). *Dlmo* may be required for either function because LIM proteins are often expressed in the nervous system and muscles (Curtiss and Heilig 1998; Dawid *et al.* 1998; Jurata and Gill 1998). Indeed, we find that in the embryo, *Dlmo* expression is restricted primarily to the CNS (M. Shoresh and D. Segal, unpublished observations).

The mutant phenotypes of lesions in the *Dlmo* gene involving wing margin defects and abnormal wing posture, as well as the limited information we have about the spatial distribution of its transcript in the wing imaginal discs and embryonic CNS, suggest that this LMO protein participates in diverse processes during development and differentiation of Drosophila. In this respect, it resembles its vertebrate homologs, which are expressed in the embryonic CNS and in the hematopoietic system and are involved in a multitude of processes during animal development (Curtiss and Heilig 1998; Dawid *et al.* 1998; Jurata and Gill 1998).

***Dlmo* may participate in a DNA-binding complex regulating wing development:** Overexpression of *Dlmo* in certain imaginal wing disc cells causes scalloping. The interactions we observe between *ap* and *Chip* mutations and their analogy to the interactions between their mammalian counterparts enable us to propose a model to explain the role of *Dlmo* in wing development. Mutations in *ap* and *Chip* cause varying degrees of wing scalloping. Studies by different groups have demonstrated that the NLI protein, of which *Chip* is a homolog, is capable of specifically binding to various LIM homeodomain proteins, and as a dimer facilitates the formation of heteromeric complexes between LIM-containing transcription factors (for reviews see Curtiss and Heilig 1998; Dawid *et al.* 1998; Jurata and Gill 1998). Likewise, in Drosophila, the *Chip*-encoded protein has been shown to bind *in vitro* the *apterous* LIM homeodomain transcription factor (Morcillo *et al.* 1997). This binding is biologically significant because flies transheterozygous for *ap* and *Chip* mutations display marked augmentation of wing scalloping (Morcillo *et al.* 1997; results presented in this article).

LMO2, the vertebrate homolog of *Dlmo*, has been recently found to serve as a bridging molecule, assembling a DNA-binding complex that includes various transcription factors (Curtiss and Heilig 1998; Dawid *et al.* 1998; Jurata and Gill 1998). For example, LMO2 is an obligatory component in the formation of an oligomeric complex that includes the zinc finger protein GATA-1 and the Tal1 and E47 basic helix-loop-helix proteins. LMO2 facilitates the binding of this complex to DNA that contains both recognition motifs for binding of bHLH proteins and GATA-1–binding sites (Visvader *et al.* 1997; Wadman *et al.* 1997). Moreover, NLI is a partner in these DNA-binding complexes and mediates their assembly. Thus, LMO2 and NLI may be general bridging modules between various transcription factors that often contain LIM domains. This could also be the case in Drosophila, where DLMO and CHIP may be responsible for the assembly of various transcription complexes. Indeed, we demonstrated that mutations in *Bx* and either *ap* or *Chip* interact to augment wing scalloping. In view of both the binding of the AP (LIM homeodomain transcription factor) and CHIP (NLI homolog) proteins to each other (Morcillo *et al.* 1997), as well as the role of LMO2 (the vertebrate homolog of *Dlmo*) in the assembly of transcription factor complexes, we propose that in Drosophila, the AP, CHIP, and DLMO proteins form a similar DNA-binding com-

plex. The identity of the genes regulated by this complex remains to be elucidated. However, some of them may be genes identified downstream of *ap* in the regulatory hierarchy of wing margin formation (Diaz-Benjumea and Cohen 1993; Blair *et al.* 1994).

In mammals, GATA-1, Tal-1, LMO2, and NLI have been shown to coexpress in erythroid cells (reviewed in Curtiss and Heilig 1998; Dawid *et al.* 1998; Jurata and Gill 1998). Loss-of-function mutations in the former three have a similar phenotype, namely failure of hematopoietic development that leads to lethality (Osada *et al.* 1995). Recent studies on oligomeric complexes involving the mammalian LMO2 and NLI have demonstrated that depending on the conditions, they may function either to facilitate or inhibit formation of the corresponding DNA-binding complexes. The balance of the different constituent molecules in these complexes appears to be important for the inhibitory or synergistic effect, as well as the presence or absence of other interacting proteins (Breen *et al.* 1998; Jurata *et al.* 1998). Likewise, we find that mutations in *ap*, *Chip*, and *Bx* cause a similar phenotype, abnormal wing morphology. Our observations on the wing phenotypes of flies carrying different doses of these three genes suggest that their interaction is sensitive to the balance between the corresponding proteins. Overexpression or underexpression of *ap* augments the wing scalloping caused by overexpression of *Dlmo*. This underscores the importance of the fine tuning of the relative levels of these proteins. Overexpression of *Lhx2*, NLI, or LMO2 in erythroid cells maintains their proliferative undifferentiated state (Wu *et al.* 1994; Visvader *et al.* 1997). We suggest that in analogy, overexpression of *Dlmo* in certain cells of the wing imaginal discs disrupts the presumptive DNA-binding complex, leading to abnormal wing development.

Overexpression of LMO genes is oncogenic: Overexpression of two human LMO genes, LMO1 and LMO2, causes neoplasia. LMO1 is disrupted by a t(11;14)(p15; q11) T cell translocation involving the TCRδ locus in T cell acute lymphoblastic leukemia, (T-ALL; Boehm *et al.* 1988). LMO2 is associated with another breakpoint (11p13) that involves a distinct TCRδ locus in T-ALL (Royer-Pokora *et al.* 1991). This breakpoint disrupts the chromosome 5′ to the coding region of LMO2 and was proposed to cause deregulation of the gene leading to leukemia (Boehm *et al.* 1991a,b). In both cases, the result of the translocation is overexpression of the LMO product. Transgenic mice targeting expression of LMO1 and LMO2 to T cells develop overt malignancies, as in T-ALL. The neoplasia likely results from disruption of the stoichiometry between the LMO proteins and the transcription factors they recruit to functional DNA-binding complexes. Interestingly, the frequency of tumor incidence was proportional to the amount of transgene expression in T cells of the transgenic mice (McGuire *et al.* 1992; Larson *et al.* 1994). Overexpression of their Drosophila homolog, *Dlmo*, which leads to abnormal wing development, may serve as an *in vivo* model for T-ALL that is amenable to genetic manipulation.

We are grateful to Bill Engels, Dale Dorsett, and the Drosophila Stock Centers at Bloomington and Bowling Green for fly strains. We thank William Mattox and Brigitte Royer-Pokora for providing clones and for sharing unpublished results. Kevin O'Hare kindly provided the genomic sequence around the *P* element at 17C2-3 in π_2, and Nick Brown provided the cDNA library. We are indebted to Dale Dorsett, Patrick Morcillo, and members of our lab for stimulating discussions. This work was supported in part by a grant from The Israel Science Foundation to D.S.

LITERATURE CITED

Agulnick, A. D., M. Taira, J. J. Breen, T. Tanaka and I. B. Dawid, 1996 Interactions of the LIM domain binding factor Ldb1 with LIM homeodomain proteins. Nature **384:** 270–272.

Abler, M. L., and P. J. Green, 1996 Control of mRNA stability in higher plants. Plant Mol. Biol. **32:** 63–78.

Altaratz, M., S. W. Applebaum, D. S. Richard, L. I. Gilbert and D. Segal, 1991 Regulation of juvenile hormone synthesis in wild-type and *apterous* mutant Drosophila. Mol. Cell. Endocrinol. **81:** 205–216.

Arber, S., and P. Caroni, 1996 Specificity of single LIM motifs in targeting and LIM/LIM interaction in situ. Genes Dev. **10:** 289–300.

Bach, I., S. J. Rhodes, R. V. Pearse, T. Heinzel and B. Gloss, 1995 P-LIM, a LIM homeodomain factor, is expressed during pituitary organ and cell commitment and synergizes with *Pit-1*. Proc. Natl. Acad. Sci. USA **92:** 720–772.

Baltz, R., J.-L. Evrard, C. Domon and A. Steinmetz, 1992 A LIM motif is present in a pollen-specific protein. Plant Cell **4:** 1465–1466.

Bernstein, S. I., P. T. O'Donnell and R. M. Cripps, 1993 Molecular genetic analysis of muscle development, structure and function in Drosophila. Int. Rev. Cytol. **143:** 63–153.

Blair, S. S., D. L. Brower, J. B. Thomas and M. Zavortnik, 1994 The role of *apterous* in the control of dorsoventral compartmentalization and PS integrin gene expression in the developing wing of Drosophila. Development **120:** 1805–1815.

Boehm, T., R. Baer, I. Lavenir, A. Forster, J. J. Waters *et al.*, 1988 The mechanism of chromosomal translocation t(11:14) involving the T-cell acceptor C delta locus on human chromosome 14q11 and a transcribed region of chromosome 11p15. EMBO J. **7:** 385–394.

Boehm, T., L. Foroni, Y. Kaneko, M. F. Perutz and T. H. Rabbitts, 1991a The rhombotin family of cysteine rich LIM domain oncogene: distinct members are involved in T-cell translocations to human chromosome 11p15 and 11p13. Proc. Natl. Acad. Sci USA **88:** 4367–4371.

Boehm, T., M. G. Spillantini, M. V. Sofroniew and T. H. Rabbitts, 1991b Developmentally regulated and tissue specific expression of mRNAs encoding the two alternative forms of the LIM domain oncogene rhombotin: evidence for thymus expression. Oncogene **6:** 695–703.

Bourgouin, C., S. E. Lundgren and J. B. Thomas, 1992 *apterous* is a Drosophila LIM domain gene required for the development of a subset of embryonic muscles. Neuron **9:** 549–561.

Breen, J. J., A. D. Agulnick, H. Westphal and I. B. Dawid, 1998 Interactions between LIM domains and the LIM domain-binding protein Ldb1. J. Biol. Chem. **273:** 4712–4717.

Brown, M. C., J. A. Perota and C. E. Turner, 1996 Identification of LIM3 as the principal determinant of Paxillin focal adhesion localization and characterization of a novel motif on Paxillin directing vinculin and focal adhesion kinase binding. J. Cell Biol. **135:** 1109–1123.

Chen, C. Y. A., and A. B. Shyu, 1995 AU-rich elements: characterization and importance in mRNA degradation. Trends Biochem. Sci. **20:** 465–470.

Cohen, B., M. E. McGuffin, C. Pfeifle, D. Segal and M. Cohen, 1992 *apterous*, a gene required for imaginal disc development in Drosophila, encodes a member of the LIM family of developmental regulatory proteins. Genes Dev. **6:** 715–729.

Crawford, A. W., and M. C. Beckerle, 1992 Purification and characterization of Zyxin, an 82000-dalton component of adherens junctions. J. Biol. Chem. **266:** 5847–5853.

Curtiss, J., and J. S. Heilig, 1997 *Arrowhead* encodes a LIM homeodomain protein that distinguishes subsets of Drosophila imaginal cells. Dev. Biol. **190:** 129–141.

Curtiss, J., and J. S. Heilig, 1998 DeLIMiting development. BioEssays **20:** 58–69.

Dawid, I. B., J. J. Breen and R. Toyama, 1998 LIM domains: multiple roles as adaptors and functional modifiers in protein interactions. Trends Genet. **14:** 156–162.

Diaz-Benjumea, F. J., and S. M. Cohen, 1993 Interaction between dorsal and ventral cells in the imaginal disc directs wing development in Drosophila. Cell **75:** 741–752.

Dorsett, D., 1990 Potentiation of a polyadenylation site by a downstream protein-DNA interaction. Proc. Natl. Acad. Sci. USA **87:** 4373–4377.

Engels, W. R., and C. R. Preston, 1984 Formation of chromosome rearrangements by *P* factors in Drosophila. Genetics **107:** 657–678.

Feuerstein, R., X. Wang, D. Song, N. E. Cook and S. A. Leibhaber, 1994 The LIM/double zinc finger motif functions as a protein dimerization domain. Proc. Natl. Acad. Sci. USA **91:** 10655–10659.

Foroni, L., T. Boehm, L. White, A. Forster, P. Sherrington *et al.*, 1992 The Rhombotin gene family encodes related LIM-domain proteins whose differing expression suggests multiple roles in mouse development. J. Mol. Biol. **226:** 747–761.

Freyd, G., S. K. Kim and H. R. Horvitz, 1990 Novel cysteine-rich motif and homeodomain in the product of *Caenorhabditis elegans* cell lineage gene *lin-11*. Nature **344:** 876–879.

Jurata, L. W., and G. M. Gill, 1998 Structure and function of LIM domains. Curr. Top. Microbiol. Immunol. **228:** 75–113.

Jurata, L. W., S. L. Pffaf and G. M. Gill, 1998 The nuclear LIM domain interactor NLI mediates homo- and heterodimerization of LIM domain transcription factors. J. Biol. Chem. **273:** 3152–3157.

Karlsson, O., S. Thor, Y. Norberg, H. Ohlsson and E. Edlund, 1990 Insulin gene enhancer binding protein *Isl-1* is a member of a novel class of proteins containing both a homeodomain and a Cys-His domain. Nature **344:** 879–882.

Lai, E. C., and J. W. Posakony, 1997 The Bearded box, a novel 3′UTR sequence motif, mediates negative post-transcriptional regulation of *Bearded* and *Enhancer of Split* complex gene expression. Development **124:** 4847–4856.

Larson, R. C., P. Fisch, T. A. Larson, I. Lavenir, T. Langford *et al.*, 1994 T cell tumors of disparate phenotype in mice transgenic for RBTN-2. Oncogene **9:** 3675–3681.

Leviten, M. W., E. C. Lai and J. W. Posakony, 1997 The Drosophila gene *Bearded* encodes a novel small protein and shares 3′UTR sequence motifs with multiple *Enhancer of Split* Complex genes. Development **124:** 4039–4051.

Lifschytz, L., and M. M. Green, 1979 Genetic identification of dominant overproducing mutations: the *Beadex* gene. Mol. Gen. Genet. **171:** 153–159.

Lindsley, D. L., and G. G. Zimm, 1992 *The Genome of Drosophila melanogaster*. Academic Press, San Diego.

Lundgren, S. E., C. A. Callahan, S. Thor and J. B. Thomas, 1995 Control of neuronal pathway selection by the Drosophila LIM homeodomain gene *apterous*. Development **121:** 1769–1773.

Mariol, M. C., T. Preat and B. Limbourrg-Bouchon, 1987 Molecular cloning of *fused*, a gene required for normal segmentation in the *Drosophila melanogaster* embryo. Mol. Cell. Biol. **7:** 3244–3251.

Mattox, W. W., and N. Davidson, 1984 Isolation and characterization of the *Beadex* locus of *Drosophila melanogaster*: a putative cis-acting negative regulatory element for the *heldup-a* gene. Mol. Cell. Biol. **4:** 1343–1353.

McGuire, E. A., R. D. Hockett, K. M. Pollock, M. F. Bartholdi, S. J. O'Brein *et al.*, 1989 The t(11:14)(p15:q11) in a T-cell acute lymphoblastic leukemia cell line activates multiple transcripts, including *Ttg-1*, a gene encoding a potential zinc finger protein. Mol. Cell. Biol. **9:** 2124–2132.

McGuire, E. A., C. E. Rintoul, G. M. Selar and S. J. Korsmeyer, 1992 Thymic expression of *Ttg-1* transgenic mice result in T-cell acute lymphoblastic leukemia/lymphoma. Mol. Cell. Biol. **12:** 4186–4196.

Morcillo, P., C. Rosen, M. K. Baylies and D. Dorsett, 1997 *Chip*, a widely expressed chromosomal protein required for segmentation and activity of a remote wing margin enhancer in Drosophila. Genes Dev. **11:** 2729–2740.

O'Hare, K., and G. M. Rubin, 1983 Structures of *P* transposable elements and their sites of insertion and excision in the *Drosophila melanogaster* genome. Cell **17:** 415–427.

Osada, H., G. Grutz, H. Alexon, A. Forster and T. H. Rabbitts, 1995 Association of erythroid transcription factors: complexes involving the LIM protein RBTN2 and the zinc-finger protein GATA-1. Proc. Natl. Acad. Sci. USA **92:** 9585–9589.

Pfaff, S. L., M. Mendelson, C. L. Stewart, T. Edlund and T. M. Jessell, 1996 Requirement for LIM homeobox gene *Isl1* in motor neuron generation reveals a motor neuron-dependent step in interneuron differentiation. Cell **84:** 309–320.

Porter, F. D., J. Drago, Y. Xu, S. S. Cheema, C. Wassif *et al.*, 1997 *Lhx2*, a LIM homeodomain gene, is required for eye, forebrain, and definitive erythrocyte development. Development **124:** 2935–2944.

Ringo, J., R. Werczberger, M. Altaratz and D. Segal, 1991 Female sexual receptivity and juvenile hormone synthesis are defective in mutants of the *apterous* gene of *Drosophila melanogaster*. Behav. Genet. **21:** 453–469.

Ross, J., 1995 mRNA stability in mammalian cells. Microbiol. Rev. **59:** 423–450.

Royer-Pokora, B., U. Loos and W. D. Ludwig, 1991 *TTG-2*, a new gene encoding a cysteine-rich protein with the LIM motif, is overexpressed in acute T-cell leukemia with the t(11:14)(p13:q11). Oncogene **6:** 1887–1893.

Sadler, I., A. W. Crauford, J. W. Michelsen and M. C. Beckerle, 1992 Zyxin and cCRP: two interactive LIM domain proteins associated with the cytoskeleton. J. Cell Biol. **119:** 1573–1587.

Sambrook, J., E. F. Fritsch and T. Maniatis, 1989 *Molecular Cloning: A Laboratory Manual*. Cold Spring Harbor Laboratory Press, Cold Spring Harbor, NY.

Sanchez-Garcia, I., and T. H. Rabbitts, 1994 The LIM domain: a new structural motif found in zinc-finger-like proteins. Trends Genet. **10:** 315–320.

Sanchez-Garcia, I., H. Alexon and T. H. Rabbitts, 1995 Functional diversity of LIM proteins: amino-terminal activation domains in the oncogenic proteins RBTN1 and RBTN2. Oncogene **10:** 1301–1306.

Schmeichel, K. L., and M. C. Beckerle, 1994 The LIM domain is a modular protein-binding interface. Cell **79:** 211–219.

Simmons, M. J., J. D. Raymond, N. A. Johnson and T. M. Fahey, 1984 A comparison of mutation rates for specific loci and chromosome regions in dysgenic hybrid males of *Drosophila melanogaster*. Genetics **106:** 85–94.

Smith, P. A., and V. G. Corces, 1991 Drosophila transposable elements: mechanisms of mutagenesis and interactions with the host genome. Adv. Genet. **29:** 229–300.

Stronach, B. E., S. E. Siegrist and M. C. Beckerle, 1996 Two muscle-specific LIM proteins in Drosophila. J. Cell Biol. **134:** 1179–1195.

Taira, M., H. Otani, J. P. Saint-Jeannet and I. B. Dawid, 1994 Role of the LIM class homeodomain protein Xlim-1 in neural and muscle induction by the Spemann organizer in Xenopus. Nature **372:** 677–679.

Taira, M., J.-L. Evrard, A. Steinmetz and I. B. Dawid, 1995 Classification of LIM proteins. Trends Genet. **11:** 431–432.

Tautz, D., and C. Pfeifle, 1989 A non-radioactive in situ hybridization method for the localization of specific RNAs in Drosophila embryos reveals a translational control of the segmentation gene *hunchback*. Chromosoma **98:** 81–85.

Thomas, U., F. Jonsson, S. A. Speicher and E. Knust, 1995 Phenotypic and molecular characterization of Ser^{D}, a mutant allele of the Drosophila gene *Serrate*. Genetics **139:** 203–213.

Thor, S., and J. B. Thomas, 1997 The Drosophila *islet* gene governs axon pathfinding and neurotransmitter identity. Neuron **18:** 397–409.

Visvader, J. E., X. Mao, Y. Fujiwara, K. Hahm and S. H. Orkin, 1997 The LIM domain binding protein Ldb1 and its partner

LMO2 act as negative regulators of erythroid differentiation. Proc. Natl. Acad. Sci. USA **94:** 13707–13712.

Wadman, I. S., H. Osada, G. G. Grutz, A. D. Agulnick, H. Westphal *et al.*, 1997 The LIN-only protein Lmo2 is a bridging molecule assembling an erythroid, DNA-binding complex which includes the Tal1, E47, GATA-1 and Ldb1/NLI proteins. EMBO J. **16:** 3145–3157.

Way, J. C., and M. Chalfie, 1988 *mec-3*, a homeobox-containing gene that specifies differentiation of the touch receptor neurons in *C. elegans*. Cell **54:** 5–16.

Wu, H.-K., H. H. Q. Heng, D. P. Siderovski, W. F. Dong, Y. Okuno *et al.*, 1994 Consistent high level expression of a human LIM/HOX gene, hLH-2 in chronic myelogenous leukemia and chromosomal localization to 9q33-341. Blood **84**(Suppl.): 295a.

Zhu, T. H., J. Bodem, E. Keppel, R. Paro and B. Royer-Pokora, 1995 A single ancestral gene of the human LIM domain oncogene family LMO in Drosophila: characterization of the Drosophila *Dlmo* gene. Oncogene **11:** 1283–1290.

Communicating editor: T. C. Kaufman